

## Transient Analysis of Functionally Graded Cylindrical Shell Under Impulse Local Loads

<sup>1</sup>Amirhossein Nezhadi, <sup>1</sup>Roslan Abdul Rahman and <sup>1</sup>Amran Ayob

<sup>1</sup>Faculty of Mechanical Engineering, Universiti Teknologi Malaysia, 81310 UTM Skudai, Johor, Malaysia.

**Abstract:** This paper is concerned the analysis of functionally graded cylindrical shell under impulse loads by using the Rayleigh-Ritz method. The mass density and modulus of elasticity of the FG cylindrical shell is assumed to vary according to a power law distribution in terms of the volume fractions of the constituents. Hamilton's principle with Rayleigh-Ritz method is used to derive the equation of motion of the FG cylindrical shell. The steady responses of forced vibration can be obtained by solving the equation of motion. The considered impulse load types are step pulse, sine pulse, triangular pulse and exponential pulse. The analytical results in special case are compared and validated using finite element method.

**Key words:** Forced vibration, Functionally Graded Cylinder, Impulse local Loads, Rayleigh-Ritz Method.

### INTRODUCTION

A functionally graded material (FGM) is usually a mixture of two material phases that material properties vary continuously and smoothly through the thickness from the surface of a ceramic to that of a metal on the other surface. There is not any mechanically weak junction or interface at FG shells because the material properties have gradual transition as a function. FGMs can offer several benefits such as minimization of stress concentration and attenuation of stress waves, improvement in the response of the structures, reduction of thermal stresses. Therefore, FGMs have got potential applications in an extensive range of engineering components which include the heat-engine components, armor plating, rocking motor casing, human implants and thermoelectric generators, just to name a few. There are some researches related to response of FG cylindrical shell under dynamic mechanical loads. Reddy's third order shear deformation theory is used to predict the transient response of simply supported FG cylindrical shell to low-velocity impact by a solid striker (Gong *et al.*, 1999). A numerical method for analyzing transient waves in FGM cylinders is presented by Han *et al.* (2001). At their numerical method, the FG shell along the wall thickness was divided into layer elements with three nodal lines. It is supposed that the material properties inside each element were changed linearly in the thickness direction. Nelson's numerical-analytical method (Nelson *et al.* 1971) was used by Han *et al.* (2002) to find a solution for guided waves in graded cylinders. In addition, modal analysis and Fourier transformation were used to offer a numerical method to analyze transient waves in FG cylindrical shells under impact point loads (Han *et al.*, 2002). Also, Elmaimouni *et al.* (2005), using the harmonic functions and Legendre polynomial, developed a numerical method to calculate guided wave propagation in a FG infinite cylinder. Next, Shaker *et al.* (2006) studied radial wave propagation and vibration in FG thick hollow cylinders. In their method, it is assumed that FG cylinder was made from many isotropic subcylinders. Each layer had constant material properties and functionally graded properties were reached by appropriate arrangement of layers in the multilayer cylinder. Afterward, a thick hollow FG cylinder with finite length subjected to impact internal pressure was presented and investigated the time histories of two dimensional wave propagation and stresses and displacements (Asgari *et al.*, 2009).

There are some works related to free vibrations of FG cylinders. Loy *et al.* (1999) and Pradhan *et al.* (2000) investigated the vibration behavior of FG cylindrical shells based on the Rayleigh-Ritz method and love's theory. It was revealed from the studies that the frequency characteristics of FG cylindrical shells are to those of isotropic shells. Reddy's higher order-order shear deformation shell theory was used by Yang and Shen (2003) to investigate dynamic instability and free vibration of FG cylindrical panels under thermo-mechanical loads consisting of a periodically pulsating and static forces in axial direction.

Then, Najafizadeh and Isvandzibaei (2007) using higher order shear deformation plate theory to study the vibration of thin FG cylindrical shells with ring supports. Next, Ansari and Darvizeh (2008) presented a general analytical approach to predict vibrational behavior of FGM shells.

A number of works has been done related to buckling and stabilities of FG cylinders. Stability of FG conical and cylindrical shells under non-periodic impulsive loading was performed by Sofiyev (2003, 2004). In addition, the stability of FG cylindrical shells under axial compressive load. Moreover, Kadoli and Ganesen

(2006) studied free vibration and linear thermal buckling analyses of FG cylindrical shells subjected to a temperature-specified boundary condition.

Despite the fact that many studies on the vibration problems of the FG cylindrical shell have been published, the transient analysis of thin FG cylindrical shell under impulse loads have to be comprehensively studied. An efficient way for calculating the forced vibration responses can be obtained. Also, it can be used in the dynamic design and vibration control of the cylindrical shell. In this study, forced vibration of cylindrical shell made of functionally graded material is investigated by using the Rayleigh-Ritz method.

**Formulation:**

Consider a FGM circular cylindrical shell, with a mean radius  $a$ , thickness  $h$ , length  $L$  with cylindrical coordinate  $(x, \theta, z)$  (Fig. 1). It is assumed that the mechanical properties of the shell is varied with a desired change of the volume fractions of the two materials in between the inner and outer surfaces. The mass density  $\rho$  and modulus of elasticity  $E$  are supposed to be in terms of a simple power law distribution and poisson's ratio  $\mu$  is supposed to be constant as follow (Matsunaga, 2008).

$$E(z) = E_M + E_{CM}V_f, \mu(z) = \mu, \rho(z) = \rho_M + \rho_{CM}V_f \quad (1)$$

Where

$$E_{CM} = E_C - E_M, \rho_{CM} = \rho_C - \rho_M, V_f = (0.5 + \frac{z}{h})^P \quad (2)$$

where  $P$  0 is the power law index and  $-h/2 \leq z \leq h/2$ . Subscript C and M refer to the ceramic and metal constituents, respectively. The value of the power law index (P) equal to zero represent fully ceramic shell and infinite P, represent a fully metallic shell. For thin cylindrical shell, the strain-displacement relationships are given by Soedel (1981).

$$\begin{aligned} \varepsilon_x &= \frac{\partial u}{\partial x} - z \frac{\partial^2 w}{\partial x^2}, & \varepsilon_\theta &= \frac{1}{a} \frac{\partial v}{\partial \theta} + \frac{w}{a} + z \left( \frac{1}{a^2} \frac{\partial v}{\partial \theta} - \frac{1}{a^2} \frac{\partial^2 w}{\partial \theta^2} \right), \\ \varepsilon_{x\theta} &= \frac{1}{a} \frac{\partial u}{\partial \theta} + \frac{\partial v}{\partial x} + z \left( -\frac{2}{a} \frac{\partial^2 w}{\partial x \partial \theta} + \frac{1}{a} \frac{\partial v}{\partial x} \right), \end{aligned} \quad (3)$$

The relationships between strains and stresses are written by

$$\begin{Bmatrix} \sigma_x \\ \sigma_\theta \\ \sigma_{x\theta} \end{Bmatrix} = \begin{bmatrix} \frac{E(z)}{(1-\mu^2)} & \frac{\mu E(z)}{(1-\mu^2)} & 0 \\ \frac{\mu E(z)}{(1-\mu^2)} & \frac{E(z)}{(1-\mu^2)} & 0 \\ 0 & 0 & \frac{E(z)}{2(1+\mu)} \end{bmatrix} \begin{Bmatrix} \varepsilon_x \\ \varepsilon_\theta \\ \varepsilon_{x\theta} \end{Bmatrix} \quad (4)$$

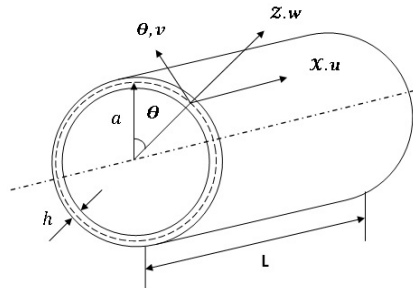


**Fig. 1:** Geometry of functionally graded cylindrical shell and coordinates.

Rayleigh-Ritz method with Hamilton's principle will be utilized to determine the equation of motion of the FG cylindrical shell. Hamilton's principle is written by

$$\int_{t_1}^{t_2} \delta(T - U)dt + \int_{t_1}^{t_2} \delta W dt = 0, \quad (5)$$

where  $T$ ,  $U$ ,  $W$  are the kinetic energy, strain energy and work,  $t_1$  and  $t_2$  are the integration time limits,  $\delta(0)$  denotes the first variation. The kinetic energy and strain energy and virtual work of a conical shell can be written as

$$U = \frac{1}{2} \int_{-h/2}^{h/2} \int_0^{2\pi} \int_0^L \{\varepsilon\}^T [S] \{\varepsilon\} a d_x d_\theta d_z \quad (6)$$

$$T = \frac{1}{2} \int_{-h/2}^{h/2} \int_0^{2\pi} \int_0^L \rho(z) \left[ \left( \frac{\partial u}{\partial t} \right)^2 + \left( \frac{\partial v}{\partial t} \right)^2 + \left( \frac{\partial w}{\partial t} \right)^2 \right] a d_x d_\theta d_z \quad (7)$$

$$\delta W = \int_0^{2\pi} \int_0^L (q_1 \delta u + q_2 \delta v + q_3 \delta w) a d_x d_\theta \quad (8)$$

where  $q_1$ ,  $q_2$  and  $q_3$  are the distributed load components per unit area along the  $x$ ,  $\theta$ , and  $z$  directions and are assumed to act on the neutral surface of the shell. The units of  $q_1$ ,  $q_2$  and  $q_3$  are  $[N/m^2]$ . The distributed loads  $q_1(t)$ ,  $q_2(t)$  are equal to zero and the FG cylindrical shell subjected to distributed radial load of  $q_3(t)$  per unit area on a localized small patch bounded by  $-\zeta_1 \leq \theta \leq \zeta_1$  and  $(\frac{L}{2} - L_2) \leq x \leq (\frac{L}{2} + L_2)$  that they are written by

$$q_1(t) = 0, q_2(t) = 0, q_3(t) = \sum_{i=1}^m \sum_{j=1}^n q_{30} F_{ij}(t) \quad (9)$$

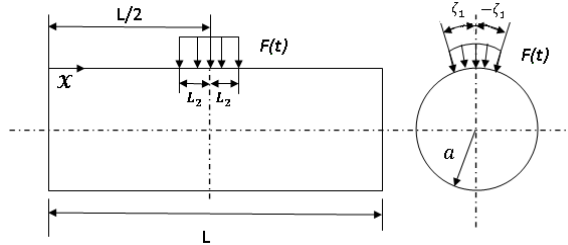


**Fig. 2:** Distributed load over small rectangular area.

$q_{30}$  is the amplitude. Substituting Eq. (9) into Eq. (8). Based on Kandasamy (2008), the work done by this load on the cylindrical shell is

$$\delta W = \int_{-\zeta_1}^{\zeta_1} \int_{\frac{L}{2}-L_2}^{\frac{L}{2}+L_2} (q_3 \delta w) a d_x d_\theta \quad (10)$$

For simply supported cylindrical shell, the boundary conditions at both ends can be written as

$$v = w = N_{11} = M_{11} = 0 \quad (11)$$

at  $x = 0$  and  $x = L$  would be considered. In order to use the Rayleigh-Ritz method, the displacement should be expressed in terms of generalized coordinates:

$$u(x, \theta, t) = \sum_{i=1}^m \sum_{j=1}^n U_{ij}(x, \theta) p_{ij}(t) = U^T(x, \theta) P(t) \quad (12)$$

$$v(x, \theta, t) = \sum_{i=1}^m \sum_{j=1}^n V_{ij}(x, \theta) r_{ij}(t) = V^T(x, \theta) r(t) \quad (13)$$

$$w(x, \theta, t) = \sum_{i=1}^m \sum_{j=1}^n W_{ij}(x, \theta) s_{ij}(t) = W^T(x, \theta) s(t) \quad (14)$$

where  $U$ ,  $V$  and  $W$  are the displacement shape functions, and  $p$ ,  $r$ ,  $s$  are the generalized coordinates or modal coordinates. They are written by

$$\begin{aligned} p &= [p_{11}, \dots, p_{1n}, p_{21}, \dots, p_{2n}, p_{m1}, \dots, p_{mn}]^T \\ r &= [r_{11}, \dots, r_{1n}, r_{21}, \dots, r_{2n}, \dots, r_{m1}, \dots, r_{mn}]^T \\ s &= [s_{11}, \dots, s_{1n}, s_{21}, \dots, s_{2n}, \dots, s_{m1}, \dots, s_{mn}]^T \\ U &= [U_{11}, \dots, U_{1n}, U_{21}, \dots, U_{2n}, \dots, U_{m1}, \dots, U_{mn}]^T \\ V &= [V_{11}, \dots, V_{1n}, \dots, V_{21}, \dots, V_{2n}, \dots, V_{m1}, \dots, V_{mn}]^T \\ W &= [W_{11}, \dots, W_{1n}, W_{21}, \dots, W_{m1}, \dots, W_{mn}]^T \end{aligned} \quad (15)$$

The principal mode shapes of cylindrical shells with simply supported boundaries can be expressed as:

$$\begin{aligned} U_{ij}(x, \theta) &= \cos\left[\frac{i\pi(x)}{l}\right] \cos(j\theta) \\ V_{ij}(x, \theta) &= \sin\left[\frac{i\pi(x)}{l}\right] \sin(j\theta) \\ W_{ij}(x, \theta) &= \sin\left[\frac{i\pi(x)}{l}\right] \cos(j\theta) \\ i &= 1, 2, \dots, m; \quad j = 1, 2, \dots, n, \end{aligned} \quad (16)$$

where  $i$  and  $j$  are the wave numbers in the meridional and circumferential directions. Substituting Eqs. (6), (7) and (10) in terms of the displacement shape functions and generalized coordinates and into Eq. (5) and performing the variation operation in terms of  $p$ ,  $r$  and  $s$ . Then, the equation of motion of the cylindrical shell can be obtained as

$$M_t \frac{d^2 X}{dt^2} + K_t X = Q, \quad (17)$$

where  $M_t$ ,  $K_t$ ,  $Q$  and  $X$  the generalized mass matrix, stiffness matrix, forcing matrix and generalized coordinate matrix and written by

$$\begin{aligned} M_t &= \begin{bmatrix} M_1 & 0 & 0 \\ 0 & M_2 & 0 \\ 0 & 0 & M_3 \end{bmatrix}, & K_t &= \begin{bmatrix} K_1 & K_2 & K_3 \\ K_2^T & K_4 & K_5 \\ K_3^T & K_5^T & K_6 \end{bmatrix} \\ Q &= [0 \ 0 \ F_{q3}q_3]^T, & X &= [p^T \ r^T \ s^T]^T \end{aligned} \quad (18)$$

where  $M_1$ ,  $M_2$  and  $M_3$  are the modal mass matrices and  $K_1, K_2, \dots, K_6$  are the modal stiffness matrices and  $F_{q3}$  is the forcing matrix which are given in Appendix A. A solution of Eq. (17) is in the form

$$X(t) = X_0 e^{\lambda t} \quad (19)$$

Where  $X_0$  is the eigenvector and  $\lambda$  is the eigenvalue. Substituting Eq. (19) into the homogeneous differential equation of Eq. (17). Then the following standard eigenvalue problem can be found:

$$(M_t \lambda^2 + K_t) X_0 = 0 \quad (20)$$

From Eq. (20) the eigenvectors and eigenvalues can be obtained. The imaginary parts of the eigenvalues are the natural frequencies of the FG cylindrical shell. Substituting Eq. (18) into Eq. (17) gives.

$$\ddot{s}_{ij}(t) + \omega_{ij}^2 s_{ij}(t) = \frac{F_{q3}q_3}{M_{3ij}} \quad (21)$$

For zero initial conditions, the solution of equation (21) will be

$$s_{ij}(t) = \frac{F_{q3}q_3 q_{30}}{M_{3ij}} \int_0^t F(\tau) \sin \omega_{ij}(t - \tau) d\tau \quad (22)$$

and the transverse displacement at any point of the cylindrical shell is given by

$$w(x, \theta, t) = \sum_{i=1}^m \sum_{j=1}^n \frac{F_{q3}q_3 q_{30}}{M_{3ij}} \sin\left[\frac{i\pi(x)}{l}\right] \cos(j\theta) \int_0^t F(\tau) \sin \omega_{ij}(t - \tau) d\tau \quad (23)$$

The convolution integral in Eqs. (22)-(23) have been solved analytically for 4 kinds of forcing functions.

$$\begin{aligned} \text{Step pulse (Fig. 3a): } F(t) &= \begin{cases} F_0, & 0 \leq t \leq t_1 \\ 0, & t > t_1 \end{cases} \\ \int_0^t F(\tau) \sin \omega_{ij}(t - \tau) d\tau &= \begin{cases} \frac{F_0}{\omega_{ij}} (1 - \cos \omega_{ij} t), & 0 \leq t \leq t_1 \\ \frac{F_0}{\omega_{ij}} (\cos \omega_{ij}(t - t_1) - \cos \omega_{ij} t), & t > t_1 \end{cases} \end{aligned} \quad (24a)$$

Sine pulse (Fig. 3b):  $F(t) = \begin{cases} F_0 \sin\left(\frac{\pi t}{t_1}\right), & 0 \leq t \leq t_1 \\ 0, & t > t_1 \end{cases}$

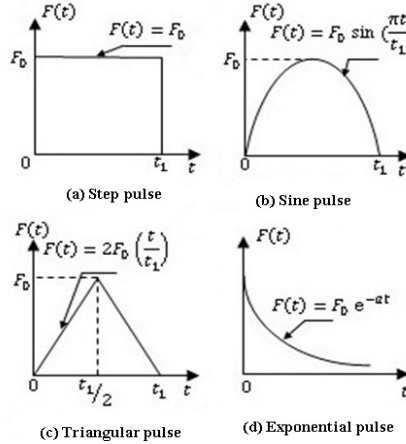


**Fig. 3:** Considered pulse shapes. (a) Step pulse. (b) Sine pulse. (c) Triangular pulse. (d) Exponential pulse.

$$\int_0^t F(\tau) \sin \omega_{ij} (t - \tau) d\tau = \begin{cases} \frac{F_0 t_1 [\pi \sin(\omega_{ij} t) - \omega_{ij} t_1 \sin(\frac{\pi t}{t_1})]}{(\pi^2 - t_1^2 \omega_{ij}^2)}, & 0 \leq t \leq t_1 \\ \frac{F_0 t_1 \pi [\sin(\omega_{ij} t) + \sin \omega_{ij} (t - t_1)]}{(\pi^2 - t_1^2 \omega_{ij}^2)}, & t > t_1 \end{cases} \quad (24b)$$

$$\text{Triangular pulse (Fig. 3c): } F(t) = \begin{cases} 2F_0 \left(\frac{t}{t_1}\right), & 0 \leq t \leq \frac{t_1}{2} \\ \frac{-4F_0 \left(t - \frac{t_1}{2}\right)}{t_1}, & \frac{t_1}{2} \leq t \leq t_1 \\ \frac{2F_0 (t - t_1)}{t_1}, & t > t_1 \end{cases}$$

$$\int_0^t F(\tau) \sin \omega_{ij} (t - \tau) d\tau = \begin{cases} \frac{2F_0}{\omega_{ij}} \left[ \frac{t}{t_1} - \frac{\sin(\omega_{ij} t)}{(\omega_{ij} t_1)} \right], & 0 \leq t \leq \frac{t_1}{2} \\ \frac{2F_0}{\omega_{ij}} \left[ 1 - \frac{t}{t_1} - \frac{\sin(\omega_{ij} t)}{(\omega_{ij} t_1)} + \frac{2 \sin \omega_{ij} (t - \frac{t_1}{2})}{(\omega_{ij} t_1)} \right], & \frac{t_1}{2} \leq t \leq t_1 \\ \frac{2F_0}{\omega_{ij}} \left[ \frac{-\sin(\omega_{ij} t)}{(\omega_{ij} t_1)} + \frac{2 \sin \omega_{ij} (t - \frac{t_1}{2})}{(\omega_{ij} t_1)} - \frac{\sin \omega_{ij} (t - t_1)}{(\omega_{ij} t_1)} \right], & t > t_1 \end{cases} \quad (24c)$$

Exponential pulse (Fig. 3d):

$$F(t) = F_0 e^{-at}, \quad 0 \leq t$$

$$\int_0^t F(\tau) \sin \omega_{ij} (t - \tau) d\tau = \begin{cases} \frac{F_0 [\omega_{ij} e^{-at} + a \sin(\omega_{ij} t) - \omega_{ij} \cos(\omega_{ij} t)]}{(a^2 + \omega_{ij}^2)}, & 0 < t \leq t_1 \\ \frac{F_0 [e^{-at_1} (\omega_{ij} \cos \omega_{ij} (t - t_1) - a \sin \omega_{ij} (t - t_1))] - F_0 [\omega_{ij} \cos(\omega_{ij} t) - a \sin(\omega_{ij} t)]}{(a^2 + \omega_{ij}^2)}, & t > t_1 \end{cases} \quad (24d)$$

## RESULTS AND DISCUSSION

The forced vibration responses of FG cylindrical shell with two simply supported boundaries are computed. The structural parameters of the FG cylindrical shell sample are:  $a = 0.4$  m and  $L = 0.4$  m.  $q_{30}$  is the amplitude of the impulse loads that equal to 4.0 MPa. It is assumed that the load applied in the radial direction over a small rectangular area:  $l_2 = 0.01$  m,  $\zeta_1 = 5.062^\circ$ . The power of exponential pulse is  $a=350$ . For this study, the duration of dynamic loads is chosen same as the natural period of the metal cylindrical shell. By numerical

calculation, it is found that the first 27 terms of Eq. (23) are sufficient to have enough accuracy. The displacement in the Z directions of the middle surface of FG cylindrical shell at position  $(L/2, 0)$  varying with time are shown in Figs. (6-7).

From Figs. (8), it is observed that there is a good agreement between the present method and finite element method. It is clear that the maximum radial deflections obtained by the two methods are approximately identical.

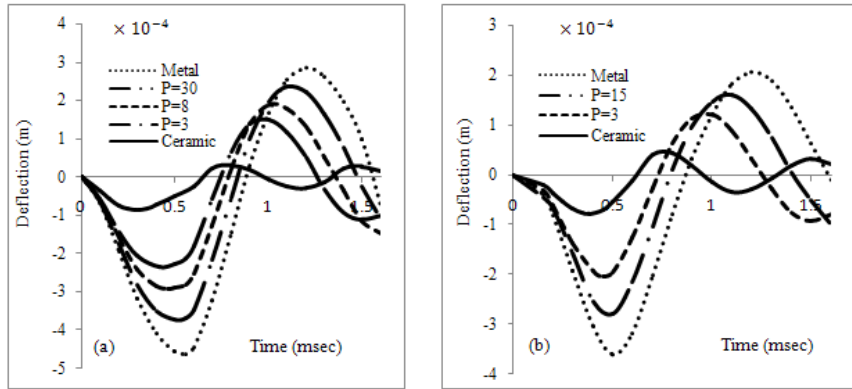


**Fig. 6:** Time response of center point deflection  $w$  for various power law indexes (P) under: (a) Step Pulse (b) Sine Pulse.

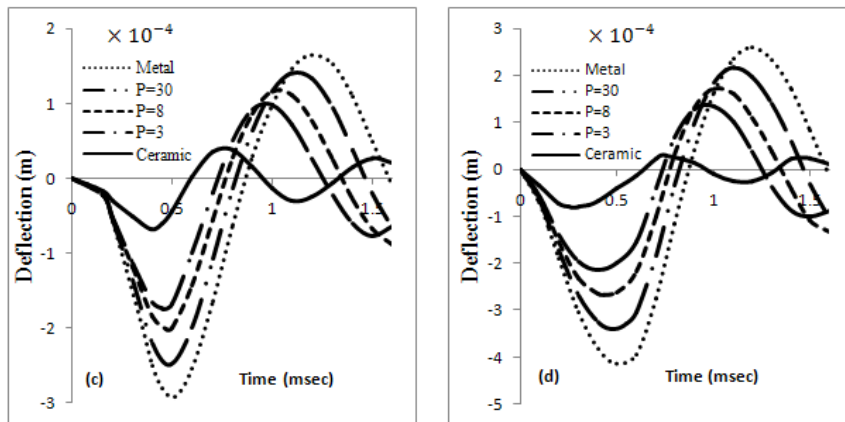


**Fig. 7:** Time response of center point deflection  $w$  for various power law indexes (P) under: (c) Triangular Pulse (d) Exponential Pulse.

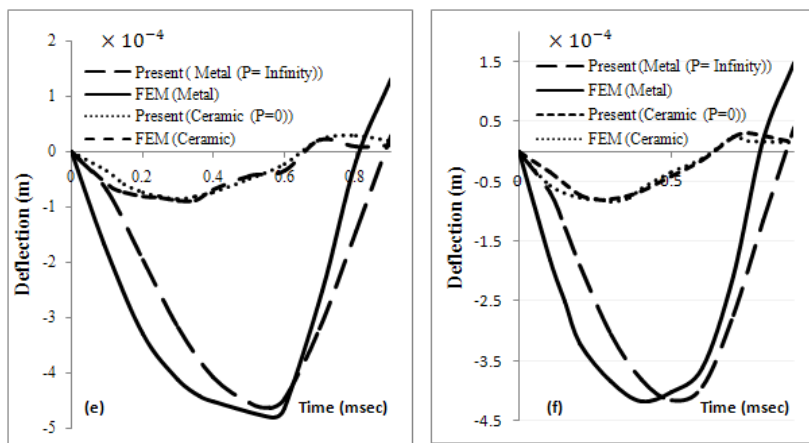


**Fig. 8:** Comparison of center deflection  $w$  with Finite Element Method under: (e) Step Pulse (f) Exponential Pulse.

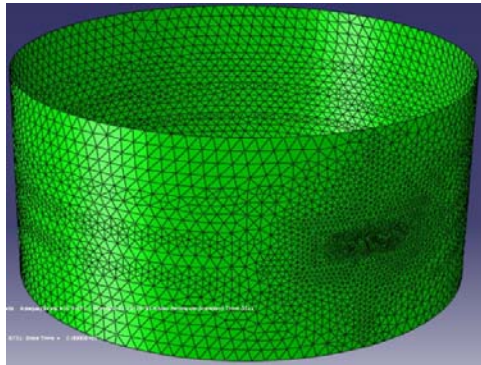


**Fig. 9:** FEM model for cylindrical shell.

The material properties used in the present study is:  
 Metal (Aluminum, Al):  $E_M = 70 \text{ GPa}$ ,  $\rho_M = 2710 \text{ kg/m}^3$ ,  $\mu = 0.3$   
 Ceramic (Almina,  $\text{Al}_2\text{O}_3$ ):  $E_C = 380 \text{ GPa}$ ,  $\rho_C = 3800 \text{ kg/m}^3$ ,  $\mu = 0.3$

It is clear from Fig. (6-7) that the largest deflection happen for metal ( $\rho = \infty$ ) under step pulse because the area below the load-time curve is greater in comparison with others pulses. When power law index ( $P$ ) increases, the corresponding time response also increases. The motions of displacement under triangular pulse are similar to the sine pulse. In addition, the maximum radial deflections of present method very close to finite element method (Fig. 8). The minimum deflections in comparison with other pulses happen under triangular pulse.

#### Appendix A:

The expressions of the modal mass, modal stiffness and forcing matrices in Eqs. (18) are given by

$$\begin{aligned}
 M_1 &= \int_0^{2\pi} \int_0^l \int_{-h/2}^{h/2} UU^T \rho(z) a \, dz \, dx \, d_\theta, \quad M_2 = \int_0^{2\pi} \int_0^l \int_{-h/2}^{h/2} VV^T \rho(z) a \, dz \, dx \, d_\theta \\
 M_3 &= \int_0^{2\pi} \int_0^l \int_{-h/2}^{h/2} WW^T \rho(z) a \, dz \, dx \, d_\theta, \\
 K_1 &= \frac{1}{1-\mu^2} \int_0^{2\pi} \int_0^l \int_{-h/2}^{h/2} \left( \frac{\partial U}{\partial x} \frac{\partial U^T}{\partial x} a \right) E(z) dz \, dx \, d_\theta + \frac{1}{a} \int_0^{2\pi} \int_0^l \int_{-h/2}^{h/2} \frac{\partial U}{\partial \theta} \frac{\partial U^T}{\partial \theta} G(z) dz \, dx \, d_\theta \\
 K_2 &= \frac{1}{1-\mu^2} \int_0^{2\pi} \int_0^l \int_{-h/2}^{h/2} \left( \mu \frac{\partial U}{\partial x} \frac{\partial V^T}{\partial \theta} \right) E(z) dz \, dx \, d_\theta + \frac{1}{2(1+\mu)} \int_0^{2\pi} \int_0^l \int_{-h/2}^{h/2} \left( \frac{\partial U}{\partial \theta} \frac{\partial V^T}{\partial x} \right) E(z) dz \, dx \, d_\theta \\
 &+ \frac{\mu}{(1-\mu^2)a} \int_0^{2\pi} \int_0^l \int_{-h/2}^{h/2} \left( \frac{\partial U}{\partial x} \right) \left( \frac{\partial V^T}{\partial \theta} \right) E(z) z dz \, dx \, d_\theta + \frac{1}{2(1+\mu)a} \int_0^{2\pi} \int_0^l \int_{-h/2}^{h/2} \left( \frac{\partial U}{\partial \theta} \right) \left( \frac{\partial V^T}{\partial x} \right) E(z) z dz \, dx \, d_\theta \\
 K_3 &= \frac{1}{1-\mu^2} \int_0^{2\pi} \int_0^l \int_{-h/2}^{h/2} \left( \mu \frac{\partial U}{\partial x} W^T \right) E(z) dz \, dx \, d_\theta - \frac{1}{(1-\mu^2)} \int_0^{2\pi} \int_0^l \int_{-h/2}^{h/2} \left( \frac{\partial U}{\partial x} \right) \left( \frac{\partial^2 W^T}{\partial x^2} \right) a E(z) z dz \, dx \, d_\theta \\
 &- \frac{\mu}{(1-\mu^2)} \int_0^{2\pi} \int_0^l \int_{-h/2}^{h/2} \left( \frac{\partial U}{\partial x} \right) \left( \frac{\partial^2 W^T}{\partial \theta^2} \right) \frac{E(z) z}{a} dz \, dx \, d_\theta - \frac{\mu}{(1-\mu^2)} \int_0^{2\pi} \int_0^l \int_{-h/2}^{h/2} \left( \frac{\partial U}{\partial x} \right) \left( \frac{\partial W^T}{\partial x} \right) E(z) z dz \, dx \, d_\theta \\
 &- \frac{2}{2(1+\mu)} \int_0^{2\pi} \int_0^l \int_{-h/2}^{h/2} \left( \frac{\partial U}{\partial \theta} \right) \left( \frac{\partial^2 W^T}{\partial x \partial \theta} \right) \frac{E(z) z}{a} dz \, dx \, d_\theta + \frac{2}{2(1+\mu)} \int_0^{2\pi} \int_0^l \int_{-h/2}^{h/2} \left( \frac{\partial U}{\partial \theta} \right) \left( \frac{\partial W^T}{\partial \theta} \right) \frac{E(z) z}{a^2} dz \, dx \, d_\theta \\
 K_4 &= \frac{1}{(1-\mu^2)} \int_0^{2\pi} \int_0^l \int_{-h/2}^{h/2} \left( \frac{\partial V}{\partial \theta} \frac{\partial V^T}{\partial \theta} \frac{1}{a} + \frac{\partial V}{\partial \theta} \frac{\partial V^T}{\partial \theta} \frac{\eta^2}{a^3} \right) E(z) dz \, dx \, d_\theta + \int_0^{2\pi} \int_0^l \int_{-h/2}^{h/2} \left( \frac{\partial V}{\partial x} \frac{\partial V^T}{\partial \theta} a \right) G(z) dz \, dx \, d_\theta \\
 &+ \int_0^{2\pi} \int_0^l \int_{-h/2}^{h/2} \left( \frac{\partial V}{\partial x} \frac{\partial V^T}{\partial x} \frac{1}{a} \right) G(z) z^2 dz \, dx \, d_\theta + \frac{2}{(1-\mu^2)} \int_0^{2\pi} \int_0^l \int_{-h/2}^{h/2} \left( \frac{\partial V}{\partial \theta} \right) \left( \frac{\partial V^T}{\partial \theta} \right) \frac{E(z) z}{a^2} dz \, dx \, d_\theta \\
 &+ \frac{2}{2(1+\mu)} \int_0^{2\pi} \int_0^l \int_{-h/2}^{h/2} \left( \frac{\partial V}{\partial x} \right) \left( \frac{\partial V^T}{\partial x} \right) E(z) z dz \, dx \, d_\theta \\
 K_5 &= \frac{1}{(1-\mu^2)} \int_0^{2\pi} \int_0^l \int_{-h/2}^{h/2} \frac{\partial V}{\partial \theta} \frac{W^T}{a} E(z) dz \, dx \, d_\theta
 \end{aligned}$$

$$\begin{aligned}
 & -\frac{1}{(1-\mu^2)} \int_0^{2\pi} \int_0^1 \int_{-h/2}^{h/2} (\mu \frac{\partial V}{\partial \theta} \frac{\partial^2 W^T}{\partial x^2} \frac{1}{a} + \frac{\partial V}{\partial \theta} \frac{\partial^2 W^T}{\partial \theta^2} \frac{1}{a^3}) E(z) z^2 d_z d_x d_\theta + 2 \int_0^{2\pi} \int_0^l \int_{-h/2}^{h/2} (-\frac{\partial V}{\partial x} \frac{\partial^2 W^T}{\partial x \partial \theta} \frac{1}{a}) G(z) z^2 d_z d_x d_\theta \\
 & + \frac{1}{(1-\mu^2)} \int_0^{2\pi} \int_0^l \int_{-h/2}^{h/2} (\frac{\partial V}{\partial \theta}) (W^T) \frac{E(z) z}{a^2} d_z d_x d_\theta - \frac{1}{(1-\mu^2)} \int_0^{2\pi} \int_0^1 \int_{-h/2}^{h/2} (\frac{\partial V}{\partial \theta}) (\frac{\partial^2 W^T}{\partial \theta^2}) \frac{E(z) z}{a^2} d_z d_x d_\theta \\
 & - \frac{\mu}{(1-\mu^2)} \int_0^{2\pi} \int_0^l \int_{-h/2}^{h/2} (\frac{\partial V}{\partial \theta}) (\frac{\partial^2 W^T}{\partial x^2}) E(z) z d_z d_x d_\theta - \frac{2}{2(1+\mu)} \int_0^{2\pi} \int_0^l \int_{-h/2}^{h/2} (\frac{\partial V}{\partial x}) (\frac{\partial^2 W^T}{\partial x \partial \theta}) E(z) z d_z d_x d_\theta \\
 K_6 = & \frac{1}{(1-\mu^2)} \int_0^{2\pi} \int_0^l \int_{-h/2}^{h/2} (\frac{\partial^2 W}{\partial x^2} \frac{\partial^2 W^T}{\partial x^2} a) E(z) z^2 d_z d_x d_\theta \\
 & + \frac{1}{(1-\mu^2)} \int_0^{2\pi} \int_0^l \int_{-h/2}^{h/2} (\frac{\partial^2 W}{\partial \theta^2} \frac{\partial^2 W^T}{\partial \theta^2} \frac{1}{a^3} + \mu \frac{\partial^2 W}{\partial x^2} \frac{\partial^2 W^T}{\partial \theta^2} \frac{1}{a} + \mu \frac{\partial^2 W}{\partial \theta^2} \frac{\partial^2 W^T}{\partial x^2} \frac{1}{a}) E(z) z^2 d_z d_x d_\theta \\
 & + \frac{1}{(1-\mu^2)} \int_0^{2\pi} \int_0^l \int_{-h/2}^{h/2} \frac{w w^T}{a} E(z) d_z d_x d_\theta + 4 \int_0^{2\pi} \int_0^l \int_{-h/2}^{h/2} (\frac{\partial^2 W}{\partial x \partial \theta} \frac{\partial^2 W^T}{\partial x \partial \theta}) \frac{G(z)}{a} z^2 d_z d_x d_\theta - \\
 & \frac{1}{(1-\mu^2)} \int_0^{2\pi} \int_0^l \int_{-h/2}^{h/2} (\frac{\partial^2 W}{\partial \theta^2}) (W^T) \frac{E(z) z}{a^2} d_z d_x d_\theta - \frac{\mu}{(1-\mu^2)} \int_0^{2\pi} \int_0^l \int_{-h/2}^{h/2} (\frac{\partial^2 W}{\partial x^2}) (W^T) E(z) z d_z d_x d_\theta \\
 & - \frac{1}{(1-\mu^2)} \int_0^{2\pi} \int_0^l \int_{-h/2}^{h/2} (W) (\frac{\partial^2 W^T}{\partial \theta^2}) \frac{E(z) z}{x^2} d_z d_x d_\theta \\
 F_{q3} = & \int_{-\zeta_1}^{\zeta_1} \int_{\frac{L}{2}-l_2}^{\frac{L}{2}+l_2} W^T a d_x d_\theta
 \end{aligned} \tag{25}$$

## REFERENCES

Ansari, R. and M. Darvizeh, 2008. "Prediction of Dynamic Behavior of FGM Shells under Arbitrary Boundary Conditions", *Composite Structures*, 85(4): 284-292.

Asgari, M., M. Akhlaghi and S.M. Hosseini, 2009. "Dynamic Analysis of Two-Dimensional Functionally Graded Thick Hollow Cylinder with Finite Length under Impact Loading", *Acta Mechanica*, 208(3-4): 163-180.

Elmimouni, L., J.E. Lefebvre, V. Zhang and T. Gryba, 2005. "Guided Waves in Radially Graded Cylinders: A Polynomial Approach", *NDT & E International*, 38(5): 344-353.

Gong, S.W., K.Y. Lam and J.N. Reddy, 1999. "Elastic Response of Functionally Graded Cylindrical shells to Low -Velocity Impact", *International Journal of Impact Engineering*, 22(4): 397-417.

Han, X., D. Xu. and G.R. Liu, 2002. "Transient Response in a Functionally Graded Cylindrical Shell to Point Load", *Journal of Sound and Vibration*, 251(5): 783-805.

Han, X., G.R. Liu, Z.C. Xi and K.Y. Lam, 2001. "Transient Waves in a Functionally Graded Cylinder", *International Journal of Solids and Structures*, 38(17): 3021-3037.

Han, X., G.R. Liu, Z.C. Xi and K.Y. Lam, 2002. "Characteristics of Waves in a Functionally Graded Cylinder", *International Journal for Numerical Methods in Engineering*, 53(3): 653-676.

Kadoli, R. and N. Ganesan, 2006. "Bckling and Free Vibration Analysis of Functionally Graded Cylindrical Shells Subjected to a Temperature-Specified Boundary Condition", *Journal of Sound and Vibration*, 289(3): 450-480.

Kandasamy, S., 2008. "Vibration Analyses of Open Shells of Revolution", Ph.D. Thesis, University of Western Ontario.

Loy, C.T., K.Y. Lam and J.N. Reddy, 1999. "Vibration of Functionally Graded Cylindrical Shells", *International Journal of Mechanical Sciences*, 41(3): 309-324.

Matsunaga, H., 2009. "Free Vibration and Stability of Functionally Graded Circular Cylindrical Shell According to a 2D Higher -Order Shear Deformation Theory", *Composite Structures*, 88: 519-531.

Najafizadeh, M.M. and M.R. Isvandzibaei, 2007. "Vibration of Functionally Graded Cylindrical Shells based on Higher Order Shear Deformation Plate Theory with Ring Support", *Acta Mechanica*, 191(1-2): 75-91.

Nelson, R.B., S.B. Dong and R.D. Kalra, 1971. "Vibrations and Waves in Laminated Orthotropic Circular Cylinders", *Journal of Sound and Vibration*, 18(3): 429-444.

Pradhan, S.C., C.T. Loy, K.Y. Lam and J.N. Reddy, 2000. "Vibration Characteristics of Functionally Graded Cylindrical Shells under Various Boundary Conditions", *Applied Acoustics*, 61(1): 111-129.

Shakeri, M., M. Akhlaghi and S.M. Hosseini, 2006. "Vibration and Radial Wave Propagation Velocity in Functionally Graded Thick Hollow Cylinder", *Composite Structures*, 76(1-2): 174-181.

Soedel, W., 1981. "Vibrations of Shells and Plates", Marcel Dekker Inc., New York.

Sofiyev, A.H., 2003. "Dynamic Buckling of Functionally Graded Cylindrical Thin Shells under Non-Periodic Impulse Loading", *Acta Mechanica*, 165(3-4): 151-163.

Sofiyev, A.H., 2004. "The Stability of Functionally Graded Truncated Conical Shells Subjected to a Periodic Impulsive Loading", International Journal of Solid and Structures, 41(13): 3411-3424.

Sofiyev, A.H., 2005. "The Stability of Compositionally Graded Ceramic-Metal Cylindrical Shells under a Periodic Axial Impulse Loading", Composite Structures, 69(2): 247-257.

Yang, J. and H.S. Shen, 2003. "Free Vibration and Parametric Response of Shear Deformable Functionally Graded Cylindrical Panels", Journal of Sound and Vibration, 261(5): 871-893.